

Crystal-field excitations in CeX_2Si_2 ($X=Au, Ag, Pd, \text{ and } Ru$)

A. Severing

*II Physikalisches Institut, Universität zu Köln, Federal Republic of Germany
and Institut Laue-Langevin, Grenoble CEDEX, France*

E. Holland-Moritz

*Institut für Festkörperforschung, Kernforschungsanlage Jülich, Federal Republic of Germany
and II Physikalisches Institut, Universität zu Köln, Federal Republic of Germany*

B. D. Rainford and S. R. Culverhouse

Physics Department, University of Southampton, Southampton, Great Britain

B. Frick

*Institut Laue-Langevin, Grenoble CEDEX, France
(Received 12 September 1988)*

In this paper we present results of thermal neutron scattering experiments on $CeAu_2Si_2$, $CeAg_2Si_2$, $CePd_2Si_2$, and $CeRu_2Si_2$. All compounds except $CeRu_2Si_2$ show distinct crystal-field excitations. We give a complete set of crystal-field parameters for the Ag, Au, and Pd compounds.

INTRODUCTION

Several groups have intensively studied the bulk properties of the CeX_2Si_2 series (X denotes a transition metal).¹⁻¹⁰ It turned out that an exchange of X from the middle range of the transition-metal row towards the noble metals changes the cerium valence from intermediate valent ($CeRu_2Si_2$) to nearly trivalent ($CeAg_2Si_2$ and $CeAu_2Si_2$). $CeAu_2Si_2$, $CeAg_2Si_2$, and $CePd_2Si_2$ order antiferromagnetically at $T_N=10$ K,¹⁰ whereas $CeRu_2Si_2$ does not show any magnetic order above 30 mK.⁵ In the Ag- and Au-based compounds the $4f$ conduction electron scattering is weaker than in $CePd_2Si_2$, but in $CePd_2Si_2$ it is still not strong enough to destroy the magnetic order as in $CeRu_2Si_2$. In $CeRu_2Si_2$ the $4f$ conduction electron scattering dominates and no magnetic order develops. This hierarchy is supported by the systematic increase of the quasielastic linewidth within the series as determined in previous neutron scattering experiments with higher energy resolution^{11,12} [$\Gamma/2(Ag) \simeq \Gamma/2(Au) < \Gamma/2(Pd) < \Gamma/2(Ru)$]. At high temperatures the quasielastic linewidth of $CeRu_2Si_2$ is even larger than in the heavy-fermion compound $CeCu_2Si_2$. At low temperatures its magnetic response changes from quasielastic to inelastic.^{11,13}

EXPERIMENT

The CeX_2Si_2 samples ($X=Au, Ag, Pd, \text{ and } Ru$) were prepared by arc melting. The x-ray diffraction pattern verified that the samples are single phase and crystallize in the tetragonal $ThCr_2Si_2$ structure ($I4/mmm$). The lattice constants agree with values reported previously.^{1,2,5}

The experiments were performed with the high-flux reactor at the Institut Laue-Langevin on the thermal beam spectrometer IN4. We used incident energies of 50,

30, and 12 meV, and the corresponding energy resolutions (FWHM) are $\Delta E=3.0, 1.8, \text{ and } 0.75$ meV, respectively. The detectors were mounted between $2\theta=10^\circ$ and $2\theta=100^\circ$ (2θ denotes the scattering angle). Background correction was determined by measurements on the empty sample holder and a cadmium plate in the sample position. The spectra shown are corrected for background scattering, absorption, and detector efficiency, with the statistical error of the spectra given by the scattering among the data points. For the data fits the magnetic form factor variation is corrected for each detector and each channel. The phonon correction was performed by measuring $LaRu_2Si_2$ as a nonmagnetic reference compound and by analyzing the Q dependence (Q denotes the momentum transfer) of the scattering response; the magnetic form factor decreases with increasing Q , whereas the phonon scattering becomes stronger with increasing Q . In addition, the magnetic form factor of a Ce^{3+} ion is well known, i.e., the Q dependence of the magnetic scattering is fixed. The Q dependence of the phonon scattering is determined via the La measurement. Fitting the low- and high- Q data consistently and taking into account the phonon scale factor from the La measurement allows the separation of the magnetic and phonon scattering. A simple subtraction of the La spectrum was not favorable because the phonon positions vary due to the different atomic weights and lattice constants. Furthermore, this method is problematic because of the different scattering lengths of the constituents, in particular the large incoherent cross section of La compared to Ce.

RESULTS AND DISCUSSION

In a crystal field (CF) with tetragonal point symmetry, the Hund's rule ground state with $J=\frac{5}{2}$ of a Ce^{3+} ($4f^1$) ion splits into three doublets. At low temperatures only

transitions from the ground state take place; hence, the neutron scattering spectra should exhibit two inelastic excitations. At higher temperatures, when the first excited state is thermally populated, the third transition should become visible.

Figure 1 shows the 50-meV spectra of CeAg_2Si_2 , CeAu_2Si_2 , CePd_2Si_2 , and CeRu_2Si_2 for two different scattering angles. The low-angle data (low Q , left side of Fig. 1) contain mainly magnetic scattering, whereas mainly phonon scattering contributes to the high-angle data (high Q , right side). The phonon scattering is marked by the hatched areas, and the dashed lines represent the magnetic scattering. The lines in the $X=\text{Ag}$, Au , and Pd are the result of quantitative CF analysis; in CeRu_2Si_2 the magnetic scattering is fitted with only one Lorentzian line (see the following). The CeAg_2Si_2 , CeAu_2Si_2 , and CePd_2Si_2 intensities are calibrated to the full Ce^{3+} cross section via

$$\sigma_{\text{mag}} = \int_{-\epsilon}^{\epsilon} S(\underline{Q}, \omega) d\omega = CF(\underline{Q})^2 \mu_{\text{loc}}^2 = 3.9 \text{ b}, \quad (1)$$

where $F(\underline{Q})$ is the local magnetic form factor and $C=0.605 \text{ b}/\mu_B^2$. $S(\underline{Q}, \omega)$ is given by

$$S(\underline{Q}, \omega) = \left[\frac{g_N r_e}{2\mu_B} \right]^2 F(\underline{Q})^2 \frac{\hbar\omega}{1 - \exp(-\hbar\omega/k_B T)} \times \chi_{\text{bulk}} P(\underline{Q}, \omega), \quad (2)$$

where χ_{bulk} is the static susceptibility $\chi(\underline{Q}=0)$ as measured in a susceptometer and $P(\underline{Q}, \omega)$ is a spectral function which fulfills

$$\int_{-\infty}^{\infty} P(\underline{Q}, \omega) d\omega = 1.$$

If $P(\underline{Q}, \omega)$ can be approximated by a δ function, i.e., if $\Gamma/2 \ll k_B T$ ($\Gamma/2$ denotes the linewidth) then the integration in Eq. (1) can be performed from $\pm\epsilon = \pm\infty$. However, in the present materials $\Gamma/2$ is larger than $k_B T$ ($\Gamma/2 \geq k_B T$) and the upper integration can only be performed numerically. In order to avoid the divergence of the integration in Eq. (1), ϵ has to be finite.¹⁴ Here a cutoff energy of $\pm\epsilon = \pm 500 \text{ meV}$ was chosen. Note the different scales when comparing the $X=\text{Ag}$, Au , and Pd spectra. The intensity scale of CeRu_2Si_2 is given in arbitrary units. For a CF analysis one has to compare intensity ratios of quasielastic and inelastic scattering. Therefore, we analyzed the magnetically ordering samples (Ag , Au , and Pd) at temperatures above the ordering transition. In the ordered state magnon scattering instead of quasielastic scattering occurs and the CF excitations are shifted by about 4% towards higher energy transfers with respect to the nonordered phase.

The spectrum of CeAg_2Si_2 shows two distinct excitations at about 9 and 18 meV. The comparison with the high- Q spectrum verifies the magnetic character of these two peaks. These transitions have to be from the ground state since at 15 K excited states are not populated. The splittings $|1\rangle \rightarrow |2\rangle$ and $|2\rangle \rightarrow |3\rangle$ are nearly equidistant, and hence at higher temperatures no third line due to the transition $|2\rangle \rightarrow |3\rangle$ is observable. The latter is demonstrated by the 12-meV spectrum of CeAg_2Si_2 at 120 K (see the upper part of Fig. 2). There the excitation at about $\pm 9 \text{ meV}$ is a mixture of the transitions $|1\rangle \rightarrow |2\rangle$ and $|2\rangle \rightarrow |3\rangle$ (see the following CF analysis).

In CeAu_2Si_2 two inelastic, magnetic excitations at about 17 and 21 meV are observed (compare low- and high- Q data in Fig. 1). The hump at about 7 meV is clearly due to phonon scattering (note the heavy mass of Au). In a 30-meV measurement both transitions are even better resolved. For the same reason as in CeAg_2Si_2 , both excitations have to be from the ground state. At higher temperatures we observed the transition $|2\rangle \rightarrow |3\rangle$ as shown in Fig. 2. Figure 2 shows a 12-meV spectrum of CeAu_2Si_2 at 150 K (see the following CF analysis).

In contrast to the Ag- and Au-based samples, the spectrum of CePd_2Si_2 exhibits only one broad, inelastic peak. A measurement with an incident energy of 30 meV at 15 K did not provide further information. The quasielastic linewidth of $\Gamma/2 \simeq 1.2 \text{ meV}$ at 30 K in CePd_2Si_2 is about six times larger than in CeAu_2Si_2 , i.e., due to the stronger $4f$ conduction electron scattering in CePd_2Si_2 the CF excitations are broadened as well. A comparison of the low- and high-angle data shows that the peak center moves towards smaller energy transfers with increasing

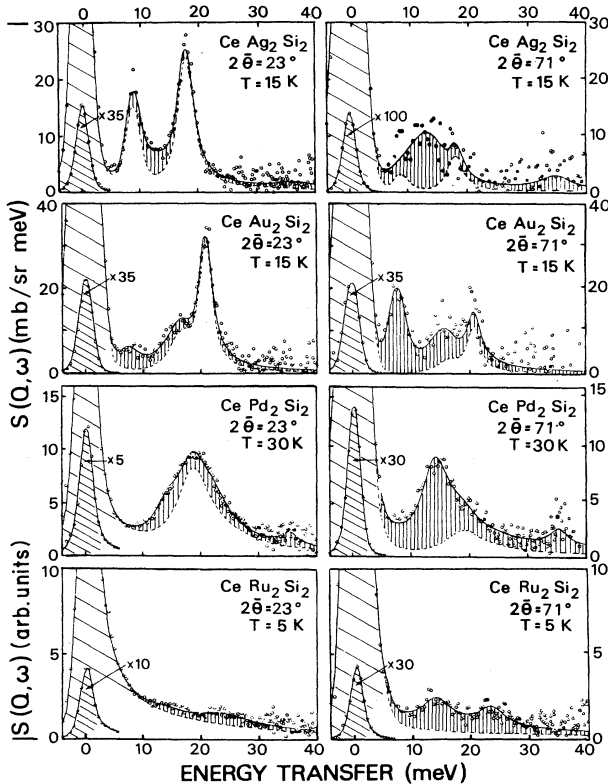


FIG. 1. 50-meV spectra of the CeX_2Si_2 compounds with $X=\text{Ag}$, Au , Pd , and Ru for low ($13.5^\circ \leq 2\theta \leq 32.6^\circ$) and high ($67.6^\circ \leq 2\theta \leq 74.3^\circ$) scattering angles. The hatched areas at zero energy transfer mark the incoherent elastic scattering. The solid lines in the Ag, Au, and Pd spectra are the result of CF analysis, for CeRu_2Si_2 see the text. The vertically dashed areas indicate the phonon contribution, the white areas underneath are the magnetic scattering.

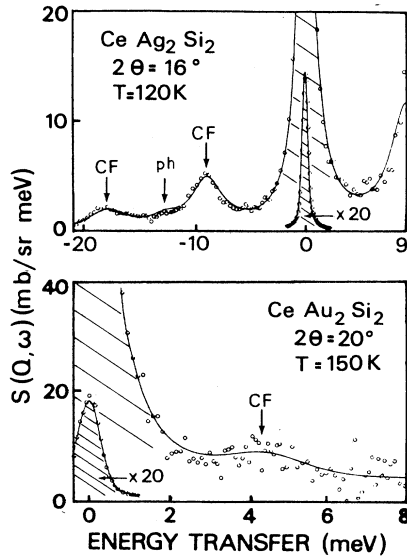


FIG. 2. 12.5-meV spectra of CeAg_2Si_2 and CeAu_2Si_2 for $7^\circ \leq 2\theta \leq 16^\circ$ and $9^\circ \leq 2\theta \leq 29^\circ$, respectively. The lines result from quantitative CF analysis. CF denotes the CF excitations and ph the phonon scattering. The neutron energy-gain side is depicted for the CeAg_2Si_2 spectrum, and the energy-loss side of the CeAu_2Si_2 spectrum shows the transition $|2\rangle \rightarrow -|3\rangle$.

Q , i.e., the low-energy tail of the peak is mainly phonon scattering, whereas the scattering around 19 meV is of magnetic origin. The assumption of nearly degenerate transitions $|1\rangle \rightarrow |2\rangle$ and $|1\rangle \rightarrow |3\rangle$ of broader intrinsic width than in CeAu_2Si_2 and CeAg_2Si_2 can explain why we did not observe a second magnetic excitation (see the following CF analysis).

The inelastic spectrum of CeRu_2Si_2 looks flat at low scattering angles. The humps centered at about 15 and 23 meV are due to phonon scattering, as a comparison with the high- Q data shows. High-resolution neutron scattering experiments¹¹ have shown that an inelastic Lorentzian describes the low-energy response of CeRu_2Si_2 better than a quasielastic line. The dashed line in Fig. 1 represents a fit with an inelastic Lorentzian line of the same position ($\hbar\omega_i = 0.82$ meV) and linewidth ($\Gamma_i/2 = 1.35$ meV) as determined from measurements with better energy resolution at the same temperature. Including the phonon correction (solid line), we obtain a satisfying fit without taking into account additional inelastic lines due to CF excitations. In Ref. 11 it is pointed out that the inelastic line centered at 0.82 meV *cannot* be explained by CF splittings. From the high-resolution data which are calibrated to absolute intensities via a vanadium standard, we obtain an intensity of the low-energy response of 1.3 b ($\pm 15\%$). This value is by a factor of 2 smaller than the full Ce^{3+} magnetic cross section (3.9 b) and leads to a reduced magnetic moment of $1.48\mu_B$. The high-temperature slope of the static susceptibility yields a magnetic moment of $2.37\mu_B$ (Ref. 5) (full Ce^{3+} moment: $2.54\mu_B$). The missing magnetic intensity strongly suggests the existence of CF excitations. The latter is supported by specific-heat⁸ and ultrasonic data¹⁵

which can be fitted with a total CF splitting between 20 and 30 meV. From this, the further possibility of a CF field splitting larger than our energy window of 45 meV can be excluded.

A possible explanation for the lack of observation of CF excitations in CeRu_2Si_2 is the following: From $X=\text{Ag, Pd, and Rh}$ to Ru (these elements are adjacent to each other in the periodic table) the $4f$ conduction electron scattering becomes stronger, which leads to CF excitations in CeRu_2Si_2 which are so broadened that they are hidden in the background. However, a comparison with earlier neutron scattering results on CeCu_2Si_2 (Ref. 16) shows that this explanation is not straightforward (Au, Ag, and Cu are above one another in the periodic table). CeCu_2Si_2 does show distinct CF excitation at about 12 and 30 meV, and its quasielastic line exhibits a width of $\Gamma/2 \approx 1$ meV at $T=5$ K. For CeRu_2Si_2 the width of the inelastic line, $\Gamma_i/2 \approx 1.35$ meV at 5 K, is a measure of the ground-state width, and this value is comparable with the one of CeCu_2Si_2 .¹¹ This rather suggests that at $T=5$ K the $4f$ conduction electron scattering in CeRu_2Si_2 and CeCu_2Si_2 is of the same order of magnitude, which should lead to a comparable CF level broadening. It might be more informative to compare the temperature slopes of the quasielastic-inelastic linewidths. In CeRu_2Si_2 the linewidth increases linearly from $T \approx 0$ K to $T=250$ K, whereas $\Gamma/2$ of CeCu_2Si_2 follows a $(a + bT^{1/2})$ law with $b < 1$ so that above $T \approx 100$ K the quasielastic linewidth of CeRu_2Si_2 is larger than in CeCu_2Si_2 . This may indicate that different mechanisms are involved causing the quasielastic-inelastic as well as the crystal-field linewidth.

So far our results are in agreement with data from Grier *et al.*¹⁷ who performed an inelastic neutron scattering experiment on powder samples using a triple-axis spectrometer. The quality of their data did not allow a quantitative analysis of the CF splittings. In the following the quantitative CF analysis of CeAg_2Si_2 , CeAu_2Si_2 , and CePd_2Si_2 will be discussed. Following Hutchings's notation,¹⁸ the CF Hamiltonian for a $J = \frac{5}{2}$ ion with tetragonal point symmetry is given by

$$H_{\text{CF}} = B_2^0 O_2^0 + B_4^0 O_4^0 + B_4^4 O_4^4$$

for c as quantization axis. The squares of the transition matrix elements and the CF transition energies can be expressed in terms of the crystal-field parameters B_2^0 , B_4^0 , and B_4^4 . However, fitting our data we used a different notation given by Walter.¹⁹ The latter is an extension of the Lea, Leask, and Wolff formalism to CF splittings in lower than cubic symmetry. Within this notation the equivalent Hamiltonian is written as

$$H_{\text{CF}} = W(x_{20} Q_2^0 + x_{40} Q_4^0 + x_{44} Q_4^4).$$

The Q_n^m are normalized CF operators O_n^m , and the normalization factors are listed in Ref. 18. Because of $\sum_{n,m} |x_{nm}| = 1$ and $\text{sgn}(x_{20}) = \text{sgn}(W)$, the three CF parameters W , x_{40} , and x_{44} describe the problem sufficiently. W roughly determines the total CF splitting and the x_{nm} determine the relative splittings and transi-

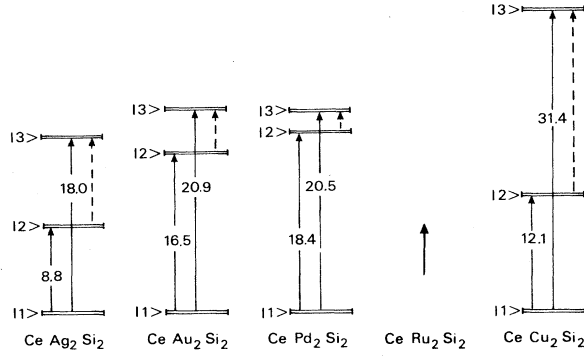


FIG. 3. CF schemes of the CeX_2Si_2 with $X = \text{Ag}, \text{Au}, \text{Pd}$, and Cu . The copper scheme is taken from Ref. 19. The arrow indicates where in the sequence the total splitting of CeRu_2Si_2 is expected.

tion matrix elements. The parameters W and x_{nm} can be simply converted into the B_n^m .¹⁹ The sign of x_{44} or B_4^4 changes the symmetry of the eigenstates, but it does not influence the squared matrix elements. Therefore we cannot distinguish between the $a|\pm\frac{3}{2}\rangle + b|\mp\frac{5}{2}\rangle$ and the $a|\pm\frac{3}{2}\rangle - b|\mp\frac{5}{2}\rangle$ state (the a and b parameters remain unchanged).

The relative intensities of the quasielastic and inelastic lines as well as the positions of the inelastic excitations are determined by the CF parameters W , x_{40} , and x_{44} . The only adjustable parameters left are the quasielastic and inelastic linewidths. However, from previous high-resolution measurements with cold incident neutrons,^{11,12} we already know the quasielastic linewidths. Therefore we did not have to vary the quasielastic linewidths; they were set to the high-resolution values. There is one peculiarity concerning CeAu_2Si_2 . In Ref. 11 it is pointed out that above the ordering transition ($T_N = 10$ K) the quasi-

TABLE II. Static bulk susceptibility χ_{bulk} from Ref. 1 and the total susceptibility, $\chi(Q)/F(Q)^2$, and van Vleck susceptibility, $\chi^{\text{VV}}(Q)/F(Q)^2$, as calculated from the magnetic neutron scattering intensities resulting from the CF analysis at the respective temperatures T .

X	T (K)	χ_{bulk} (emu/mol)	$\chi(Q)/F(Q)^2$ (emu/mol)	$\chi^{\text{VV}}(Q)/F(Q)^2$ (emu/mol)
Ag	15	0.018	0.017	0.006
Au	15	0.032	0.039	0.005
Pd	30	0.009	0.011	0.003

elastic scattering contains a Lorentzian and a non-negligible Gaussian contribution ($I_{\text{Gauss}}/I_{\text{Lor}} \simeq 1.8$). The latter was attributed to critical fluctuations preceding the magnetic order and is taken into account for the CF analysis. For particular sets of W , x_{40} , and x_{44} , we obtained good fits to the data at low- and high-scattering angles, including the phonon correction as already described (see the solid lines in Fig. 1). The dashed lines in Fig. 1 reflect the pure magnetic scattering as given by the W , x_{40} , and x_{44} parameters. In Fig. 3 the corresponding CF schemes are shown, and in Table I the CF parameters (for convenience the B_n^m are given as well) and the eigenstates are listed. The 12-meV spectra of CeAg_2Si_2 and CeAu_2Si_2 at 120 K and 150 K, respectively, could be fitted with the same CF parameters as the 50-meV spectra at low temperatures (see the solid line in Fig. 2), only the inelastic linewidths had to be varied because of the broadening with increasing temperature. The first and second excited states in CePd_2Si_2 are exchanged in comparison to the other CeX_2Si_2 compounds. This might be due to the larger uncertainty in the data analysis of the CePd_2Si_2 spectra which is caused by the broader excitation spectrum (the transitions $|1\rangle \rightarrow |2\rangle$ and $|1\rangle \rightarrow |3\rangle$ are not resolved).

TABLE I. Crystal-field parameters W , x_{40} , and x_{44} and the corresponding B_2^0 , B_4^0 , and B_4^4 as determined from the CF analysis. The W and B_n^m parameters are given in meV. The $|1\rangle$, $|2\rangle$, and $|3\rangle$ represent the eigenstates of the ground state, first excited state, etc. The a and b parameters are the factors of the $|\pm\frac{3}{2}\rangle$ and $|\pm\frac{5}{2}\rangle$. The CeCu_2Si_2 values are taken from Ref. 20. In the last line the unit-cell volumes of the CeX_2Si_2 ($X = \text{Ag}, \text{Au}, \text{Pd}$, and Cu) are listed in \AA^3 .

	CeAg_2Si_2	CeAu_2Si_2	CePd_2Si_2	CeCu_2Si_2
W	-4.3 ± 0.2	-6.4 ± 0.3	-6.1 ± 0.3	-9.3 ± 0.1
x_{40}	0.043 ± 0.01	-0.26 ± 0.02	0.001 ± 0.002	-0.22 ± 0.07
x_{44}	0.933 ± 0.09	0.70 ± 0.04	0.53 ± 0.10	0.70 ± 0.05
B_2^0	-0.04 ± 0.11	-0.09 ± 0.10	-0.95 ± 0.22	-0.26 ± 0.10
B_4^0	-0.003 ± 0.001	0.028 ± 0.003	-0.0001 ± 0.0002	0.034 ± 0.01
B_4^4	-0.33 ± 0.03	-0.38 ± 0.03	-0.27 ± 0.06	-0.54 ± 0.04
a	0.730	0.604	0.899	0.83
b	0.684	0.797	0.437	0.56
$ 3\rangle$	$b \pm\frac{5}{2}\rangle - a \mp\frac{3}{2}\rangle$	$b \pm\frac{5}{2}\rangle - a \mp\frac{3}{2}\rangle$	$ \pm\frac{1}{2}\rangle$	$b \pm\frac{5}{2}\rangle - a \mp\frac{3}{2}\rangle$
$ 2\rangle$	$ \pm\frac{1}{2}\rangle$	$ \pm\frac{1}{2}\rangle$	$b \pm\frac{5}{2}\rangle - a \mp\frac{3}{2}\rangle$	$ \pm\frac{1}{2}\rangle$
$ 1\rangle$	$a \pm\frac{5}{2}\rangle + b \mp\frac{3}{2}\rangle$	$a \pm\frac{5}{2}\rangle + b \mp\frac{3}{2}\rangle$	$a \pm\frac{5}{2}\rangle + b \mp\frac{3}{2}\rangle$	$a \pm\frac{5}{2}\rangle + b \mp\frac{3}{2}\rangle$
V	192.55	190.17	177.62	167.34

In order to prove the CF analysis we compare the resulting quasielastic and inelastic intensities with the static bulk susceptibility χ_{bulk} . Although the data are calibrated to the full Ce^{3+} cross section via integration [see Eq. (1)], this is a sensible comparison because the inelastic

scattering contributes to the static susceptibility weighted by a factor $1/\Delta_{jk}$ (Δ_{jk} is the transition energy from $|j\rangle \rightarrow |k\rangle$). This becomes apparent when rewriting Eq. (2) explicitly for a CF split system:²¹

$$S(\underline{Q}, \omega) = \left[\frac{g_N r_e}{2\mu_B} \right]^2 F(\underline{Q})^2 \frac{\hbar\omega}{1 - \exp(-\hbar\omega/k_B T)} \sum_j [\chi_{jj}^C(\underline{Q}) P_{jj}(\underline{Q}, \omega)] + \frac{1}{2} \sum_{\substack{j,k \\ j \neq k}} [1 - \exp(-\Delta_{jk}/k_B T)] [\chi_{jk}^{VV} P_{jk}(\underline{Q}, \omega)]$$

and

$$\chi_{jj}^C(\underline{Q}) \simeq 1/T |\langle j | J_z | j \rangle|^2, \quad \text{Curie contribution,}$$

$$\chi_{jk}^{VV}(\underline{Q}) \simeq 1/\Delta_{jk} |\langle j | J_z | k \rangle|^2, \quad \text{van Vleck contribution.}$$

Therefore one can prove via the static susceptibility whether or not the CF analysis yields sensible intensity ratios. In Table II the susceptometer values χ_{bulk} ,¹ the total static susceptibilities $\chi(\underline{Q})$ (the sum over the Curie and van Vleck contributions) divided by $F(\underline{Q})^2$, and the total van Vleck contribution $\chi^{VV}/F(\underline{Q})^2$ (the sum over all van Vleck terms) are listed for the respective temperatures. The agreement between χ_{bulk} and $\chi(\underline{Q})/F(\underline{Q})^2$ is satisfying. For the Au sample the Gaussian contribution of the quasielastic line is taken into account.

In Table I and Fig. 3 the CF parameters of $CeCu_2Si_2$ as given in Ref. 19 are included for comparison. The total CF splitting increases from Ag, Au, and Pd to Cu. It is intriguing that the unit-cell volumes decrease in the same way as the total CF splittings increase (see the bottom of Table I). The unit-cell volume of 171.699 \AA^3 of $CeRu_2Si_2$

lies between the values of $X=Pd$ and $X=Cu$. Therefore we expect the total crystal-field splitting ΔE_{CF} in $CeRu_2Si_2$ to be smaller than in the Cu compound but larger than in $CePd_2Si_2$ (see the arrow in Fig. 3).

CONCLUSION

The inelastic neutron scattering spectra of $CeAg_2Si_2$, $CeAu_2Si_2$, and $CePd_2Si_2$ exhibit distinct CF excitations, and we determined the crystal-field schemes and crystal-field parameters. The resulting magnetic intensities reproduce the static bulk susceptibility. The total CF splitting of the CeX_2Si_2 compounds increases in the sequence $Ag \rightarrow Au \rightarrow Pd \rightarrow Cu$, i.e., the splitting increases with decreasing unit-cell volume. We did not observe CF excitations in $CeRu_2Si_2$, but the missing magnetic intensity strongly suggests their existence. An estimation from the unit-cell volume of $CeRu_2Si_2$ leads us to expect a total CF splitting which is smaller than in $CeCu_2Si_2$ but larger than in $CePd_2Si_2$, i.e., it should be within the energy window of investigation.

¹V. Murgai, S. Raan, L. C. Gupta, and R. D. Parks, in *Valence Instabilities*, edited by P. Wachter and H. Boppert (North-Holland, Amsterdam, 1982), p. 537.

²C. Godart, L. C. Gupta, and M. F. Ravet-Krill, *J. Less-Common Met.* **94**, 187 (1983).

³J. D. Thompson, R. D. Parks, and H. Borges, *J. Magn. Magn. Mater.* **54-57**, 377 (1986).

⁴A. Amato and J. Sierro, *J. Magn. Magn. Mater.* **47&48**, 526 (1985).

⁵L. C. Gupta, D. E. MacLaughlin, Cheng Tien, C. Godart, M. A. Edwards, and R. D. Parks, *Phys. Rev. B* **28**, 3673 (1983).

⁶J. Flouquet, P. Haen, F. Lapiere, D. Jaccard, and G. Remenyi, *J. Magn. Magn. Mater.* **54-57**, 322 (1986).

⁷J. D. Thompson, J. O. Willis, C. Godart, D. E. MacLaughlin, and L. C. Gupta, *J. Magn. Magn. Mater.* **47&48**, 281 (1985).

⁸M. J. Besnus, J. P. Kappler, P. Lehmann, and A. Mayer, *Solid State Commun.* **55**, 779 (1985).

⁹F. Steglich, U. Rauchschwalbe, U. Gottwick, H. M. Mayer, G. Sporn, N. Grewe, U. Poppe, and J. J. M. Franse, *J. Appl. Phys.* **57**, 3054 (1985).

¹⁰B. H. Grier, J. M. Lawrence, V. Murgai, and R. D. Parks,

Phys. Rev. B **29**, 2664 (1984).

¹¹A. Severing, E. Holland-Moritz, and B. Frick, *Phys. Rev. B* (to be published).

¹²B. D. Rainford and S. R. Culverhouse (unpublished).

¹³W. A. C. Erkelens, Ph.D. thesis, Rijksuniversiteit Leiden, 1987.

¹⁴E. Holland-Moritz, *J. Magn. Magn. Mater.* **47&48**, 127 (1985).

¹⁵D. Weber and B. Luethi (unpublished).

¹⁶S. Horn, E. Holland-Moritz, M. Loewenhaupt, F. Steglich, H. Scheuer, A. Benoit, and J. Flouquet, *Phys. Rev. B* **23**, 3171 (1981).

¹⁷B. H. Grier, J. M. Lawrence, S. Horn, and J. D. Thompson, *J. Phys. C* **21**, 1099 (1988).

¹⁸M. T. Hutching, in *Solid State Physics*, edited by F. Seitz and B. Turnbull (Academic, New York, 1965), Vol. 16, p. 227.

¹⁹U. Walter, *J. Phys. Chem. Solids* **45**, 401 (1984).

²⁰E. Holland-Moritz, W. Weber, A. Severing, E. Zirngiebl, H. Spille, B. Baus, S. Horn, A. P. Murani, and F. Douchin, *Phys. Rev. B* (to be published).

²¹E. Holland-Moritz, D. Wohlleben, and M. Loewenhaupt, *Phys. Rev. B* **25**, 7482 (1982).